Chemical Communications

Supporting Information

A trade-off between ligand coating and crystallinity of Gd doped ultrasmall CeO_2 for improving relaxivity

Qian Ma,[1] Hui Wang,[1] Qiangqiang Nie,[2] Suying Xu,[1]* Leyu Wang[1]*

[1]*State Key Laboratory of Chemical Resource Engineering, College of Chemistry, Beijing University of Chemical Technology, Beijing 100029, China.*

[2]*Department of Cardiovascular Surgery, China-Japan Friendship Hospital*

**To whom correspondence should be addressed: State Key Laboratory of Chemical Resource Engineering, College of Chemistry, Beijing University of Chemical Technology, Beijing 100029, China*

E-mail: lywang@mail.buct.edu.cn; syxu@mail.buct.edu.cn

Table of content

Chemicals and Reagents

All the reagents were of analytical grade and used as received without further purification. Cerium (III) nitrate hexahydrate ($Ce(NO_3)_3 \cdot 6H_2O$) and gadolinium (III) nitrate hexahydrate ($Gd(NO_3)_3 \cdot 6H_2O$) were all from Beijing Chemical Reagent Company Ltd. 1,2-dimethylbenzene was purchased from aladdin. Oleylamine (OAm) was obtained from Acros Organics. Oleic acid (OA) was purchased from Alfa Aesar. Polysuccinimide (PSI, $M_w \sim 6000$) was obtained from Shijiazhuang Desai Chemical Technology Company Ltd. Chloroform, ethanol, methanol, N,N'-dimethylformamide (DMF), dimethyl sulfoxide (DMSO), NaOH, HCl (12 M) and hydrogen peroxide (H_2O_2, 30%) were all brought from Beijing Chemical Reagent Co. Ltd. Tris and tris-HCl were supplied by Beijing Kebio Biotechnology Co. Ltd. 3,3',5,5'-tetramethylbenzidine (TMB), 5,5-dimethyl-1-pyrroline N-oxide (DMPO), 2',7'-dichlorodihydrofluorescein diacetate (DCFH-DA) were purchased from Beijing InnoChem Science & Technology Co. Ltd. For cell culture, Dulbecco's modified Eagle medium (DMEM) was purchased from Hyclone. Fetal calf serum (FBS) was obtained from Hangzhou Sijiqing Bioengineer Materials Ltd. Trypsin and penicillin-Streptomycin Solution were obtained from Beijing Kebio Biotechnology Co. Ltd. Phosphate buffered saline (PBS) was acquired from Wuhan Servicebio Co. Ltd. 3-(4,5-Dimethylthiazol-2-yl)-2,5- diphenyltetrazolium bromide (MTT) was supplied by Amresco. Ultrapure water was made by a MilliQ water purification system from Millipore (Bedford, MA, USA).

Characterization and Instrument.

The transmission electron microscope (TEM) images were obtained by using JEOL JEM-1200EX (100 kV) and JEM-2100F HRTEM (200 kV). Dynamic light scatter (DLS) particle size analysis and zeta potential tests were performed by a Malvern dynamic laser scattering instrument (Zetasizer Nano-ZS90). The X-ray diffraction (XRD) patterns were collected at room temperature on a Bruker AXS D8-Advanced X-ray diffractometer. Electro spin response (ESR) spectrum was from a Bruker EMX500-10/12 spectrometer, where 5,5-dimethyl-1-pyrroline N-oxide (DMPO) was used as the spin trap to capture the produced ROS. The absorption spectrums were performed on a Shimadzu UV-3600 spectrometer. The metal composition of the samples was detected on an inductively coupled plasma optical emission spectrometer (ICP-OES, Thermo Scientific iCAP 6300 series). The cell cytotoxicity test was measured by a Tecan Infinite F50 plate reader. Cell imaging was obtained by a model eclipse Ti2−U inverted fluorescence microscope (Nikon). The longitude relaxation times (T_1) were recorded on a Bruker Avance-III 400 MHz (9.4 T) spectrometer and a 7.0 T Bruker BioSpec70/20USR MRI system. All the ^1H MRI experiments were performed on a 7.0 T Bruker BioSpec70/20USR MRI system. All PA experiments were performed by a Spectral photoacoustic tomography system (in Vision 256 TF).

Experimental Section

Synthesis of different morphology of CeO_2 materials. The CeO_2 materials with different morphology were prepared according the two-phase solvothermal method. Briefly, 22 mg of $Ce(NO_3)_3 \cdot 6H_2O$ was dissolved in 8 mL mixing solution containing 3 mL of 1,2-dimethylbenzene and 5 mL of OAm following the addition of 1 mL OA for the formation of ultrasmall CeO_2 nanodots. After stirring for 30 min, 1 mL of ultrapure water was added into the solution. The solution was transferred to a poly(tetrafluoroethylene) reactor after mixed well and then reacted for 1h at 140 °C. The solution was cooled to room temperature and precipitated with moderate ethanol. CeO_2 NDs

were acquired by centrifugation at 12000 rpm for 6 min. The NDs were redispersed in 1 mL $CHCl_3$ for later use.

Morphology regulation was realized by adjusting the adding amount of OA: 0 mL for nanowires, 100 μL for nanowires, and 1 mL for nanodots.

Synthesis of ultrasmall Gd-doped CeO_2 (CeO_2:Gd) NDs. CeO_2:Gd NDs were prepared according the above method of CeO_2 NDs without Gd doping (CeO_2: Gd(0%) NDs). Typically, 22 mg of $Ce(NO_3)_3 \cdot 6H_2O$ and 0.55/1.1/2.8 mg of $Gd(NO_3)_3 \cdot 6H_2O$ were dissolved in 8 mL mixing solution containing 3 mL of 1,2-dimethylbenzene and 5 mL of OAm following the adding of 1 mL OA. After stirring for 30 min, 1 mL of ultrapure water was added into the solution. The solution was transferred to a poly(tetrafluoroethylene) reactor after mixed well and then reacted for 1h at 100 °C / 120 °C / 140 °C / 160 °C. The solution was cooled to room temperature and precipitated with moderate ethanol. CeO_2: Gd NDs were acquired by centrifugation at 12000 rpm for 6 min. The NDs were dispersed in 1 mL $CHCl_3$ for later use.

The adding amount of $Gd(NO_3)_3 \cdot 6H_2O$ corresponded to the different doping amount of Gd^{3+} in CeO_2: Gd NDs as 0.55 mg corresponding to 1.5% (CeO_2:Gd(1.5%)), 1.1 mg corresponding to 3% (CeO_2: Gd(3.0%)) and 2.8 mg corresponding to 7.5% (CeO_2: Gd(7.5%)). The actual Gd^{3+} composition of CeO_2:Gd NDs with different Gd doping amounts were respectively 2.08%, 3.48% and 5.90% according to the ICP tests.

Synthesis of PSI_{OAm}. OAm grafted PSI (PSI_{OAm}) was synthesized according to our previous method.[1, 2] Typically, 1.6 g of PSI was dissolved in 32 mL DMF at 90 °C with magnetic stirring for 30 min. After the addition of 550 μL OAm, the solution was heated to 100 °C and kept for 5 h. Then, the solution was cooled to room temperature and totally precipitated with methanol. PSI_{OAm} was acquired by centrifugation at 7000 rpm for 4 min and dried for later use.

Fabrication of CeO_2:Gd@PSI_{OAm} and CeO_2:Gd(3.0%)-TMB@PSI_{OAm}. For the fabrication of the CeO_2:Gd(0%)@PSI_{OAm}, the CeO_2:Gd(0%) NDs was transferred to water from the hydrophobic phase by using PSI_{OAm}, according to our previous work.[1, 2] Briefly, 500 μL of CeO_2:Gd(0%) NDs stored colloids and another 500 μL of $CHCl_3$ constituted the hydrophobic phase while 10 mg of PSI_{OAm} dissolved in 10 mL of NaOH aqueous solution (20 mM) as the aqueous phase. After the hydrophobic phase was added into the aqueous phase rapidly, the mixed solution was dealt with ultrasonication at 400 W for 6 min following 4 h of magnetic stirring at 45 °C. The CeO_2:Gd(0%)@PSI_{OAm} solution can be used directly after cooling to room temperature without further treatment.

The fabrication of CeO_2:Gd@PSI_{OAm} with other Gd doping amounts was similar as CeO_2:Gd(0%)@PSI_{OAm} while replacing CeO_2:Gd(0%) NDs with CeO_2:Gd(1.5%), CeO_2:Gd(3.0%) and CeO_2:Gd(7.5%) NDs.

The CeO_2:Gd(3.0%)-TMB@PSI_{OAm} was prepared with the same method as mentioned above. Typically, the water phase was identical while the hydrophobic phase was formed by 500 μL of CeO_2:Gd(3.0%) NDs, 100 μL of TMB (5 mg/mL in $CHCl_3$) and 400 μL $CHCl_3$. After the hydrophobic phase was added into the aqueous phase rapidly, the mixed solution was dealt with ultrasonication at 400 W for 6 min following 4 h of magnetic stirring at 45 °C. The CeO_2:Gd(3.0%)-TMB @PSI_{OAm} solution can be used directly after cooled to room temperature without further treatment.

Preparation of bare CeO_2:Gd NDs. In order to exclude the effect of ligands on the surface of NDs, we have removed the OAm and OA on the NDs with acid-ethanol mixing solution. Briefly, 112 μL of HCl (12 M) was added into 15 mL ethanol before 10 mg of CeO_2:Gd NDs was dispersed. The NDs without ligands was acquired by centrifugation at 12000 rpm for 10 min after ultrasonication about 30 min. Finally, the NDs were redispersed in 1 mL of ultrapure water for later test.

The relaxation performance test and the measurement of r_1. The T_1 of different concentrations of NDs without any ligands and CeO_2:Gd@PSI_{OAm} with different Gd doping amounts or different temperatures were recorded on a Bruker Avance-III 400 MHz (9.4 T) spectrometer and a 7.0 T Bruker BioSpec70/20USR MRI system. The $1/T_1$ values were fitted linearly to the concentrations to evaluate the relaxation performance of the materials. The formula is as follows.

$$1/T_1 = 1/T_w + r_1\,[\mathrm{Gd}]$$

ROS generation of CeO_2: Gd(0%)@PSI_{OAm} and CeO_2:Gd(3.0%)@PSI_{OAm} and cell imaging. The TMB assay was conducted to evaluate ROS generation of CeO_2:Gd(0%)@PSI_{OAm} and CeO_2:Gd(3.0%)@PSI_{OAm}. TMB without color could be oxidized by ROS to show an obvious blue and enhanced absorption at 630-650 nm. CeO_2:Gd(0%)@PSI_{OAm} and CeO_2:Gd(3.0%)@PSI_{OAm} solution with same concentration of Ce of 40 μM were cultured with H_2O_2 (1 mM) and TMB (0.1 mg/mL) in Tris-HCl buffer with different pH values (pH = 5.5, 6.0, 6.5, 7.0, 7.4 and pH = 7.4 without H_2O_2) under 37 °C, respectively. The absorption of different time was recorded by UV-3600 spectrometer.

To prove the ROS generation capacity in 4T1 cells, DCFH-DA probe which can be oxidized by intracellular ROS to give out a green fluorescence was used. The 1×10^5 per well cells were seeded in a 6-wells plate and incubated at 37 °C under 5% CO_2 for 24 h to ensure the cells were adherent. Then CeO_2:Gd(0%)@PSI_{OAm} and CeO_2:Gd(3.0%)@PSI_{OAm} with same concentration of Ce of 40 μM were added to generate ROS as PBS was used as control. After being cultured for 3 h and 6 h respectively, the supernatant was removed and 2 mL of PBS was added to wash the cells and removed, which was repeated two times. Then the cells were stained with 1 mL of DCFH-DA probe (10 μM) for 20 min and observed under a fluorescent microscope.

To distinguish the species of the ROS, the spin trapping agent, DMPO, was used to capture the ROS to show a specific spectrum according the ESR system.

Cell cytotoxicity of CeO_2:Gd(3.0%)-TMB@PSI_{OAm}. The MTT assay was conducted to evaluate the cell cytotoxicity of CeO_2:Gd(3.0%)-TMB@PSI_{OAm}. Briefly, HUVECs were cultured in DMEM containing 1% penicillin-streptomycin solution and 10% FBS. Then 2×10^4 per well cells were seeded in a 96-wells plate and incubated at 37 °C under 5% CO_2 for 24 h to ensure the cells were adherent. Further, the cells were incubated at 37 °C under 5% CO_2 for 24 h or 48 h with different concentration of CeO_2:Gd(3.0%)-TMB@PSI_{OAm}. Then, 20 μL of MTT (5 mg/mL PBS) was added into each well for continuing incubation for 4 h. Finally, the supernatant was removed and 120 μL of DMSO was added into each well to dissolve the violet formazan crystal produced by viable cells. The cell viability was positive correlation with the absorption at 492 nm of the violet solution.

***In vitro*/*vivo* MRI.** Both *in vitro* and *in vivo* T_1-weighted ^{1}H MRI tests were conducted on a 7.0 T Bruker BioSpec70/20USR MRI system. For MRI test in tube, the T_1-RARE sequence was applied and the related parameters were set as follows: matrix size was 200 × 200; T_R and T_E were 300.0

and 5.01 ms, respectively; and the field of view was set at 35 mm × 35 mm with a slice thickness of 1 mm. For *in vivo* MRI, the T_1-RARE sequence was applied and the related parameters were set as follows: matrix size was 200 × 200; T_R and T_E were 384.64 and 5.0 ms, respectively; and the field of view was set at 35 mm × 35 mm with a slice thickness of 1 mm. The total experiment time was 1 min 28 s.

***In vitro*/*vivo* PAI.** Both *in vitro* and *in vivo* PA imaging tests were conducted on a Spectral photoacoustic tomography system (in Vision 256 TF). For *in vitro* PA imaging, different concentrations of CeO_2:Gd(3.0%)-TMB@PSI_{OAm} were scanned under 680 nm after cultured with 0.5 mM H_2O_2 in Tris-HCl buffer (pH 7.4/6.5) for 30 min. For *in vivo* PA imaging, the CeO_2:Gd(3.0%)-TMB@PSI_{OAm} solution was intravenously injected into mice under the scan of 680 nm at different time.

Tumor model. The four weeks female BALB/c mice (16-18 g) were obtained from SPF (Beijing) Biotechnical Co., Ltd. All animals experiments complied the relevant laws and institutional guidelines of China-Japan Friendship Hospital. All the mice were housed groupedly in cages with woodchip bedding and the standard supply of water and fodder. The breeding environment was kept clean with a regular 12 h/12 h light/dark cycle. The 4T1 cells was inoculated on the right leg of the mice with 100 μL PBS containing 1×10^6 cells. As the tumors grew up to 200-250 mm^3, the mice were intravenously injected with nanoparticle colloidal solution.

Supplementary Figures and Discussion

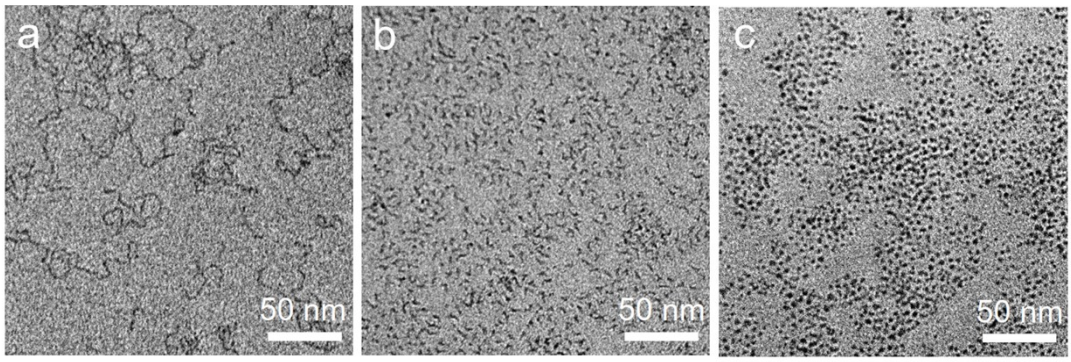

Fig. S1. TEM imaging of three morphology CeO_2 nanomaterials, i.e. CeO_2 nanowires (a), CeO_2 nanoworms (b) and CeO_2 nanodots (c).

The morphology of CeO_2 could be evolved from ultrathin nanowires to ultrasmall nanodots (NDs) by adjusting the amount of OA as revealed transmission electron microscope (TEM) images of CeO_2 nanowires, nanowroms and nanodots, respectively presented by **Fig. S1**.

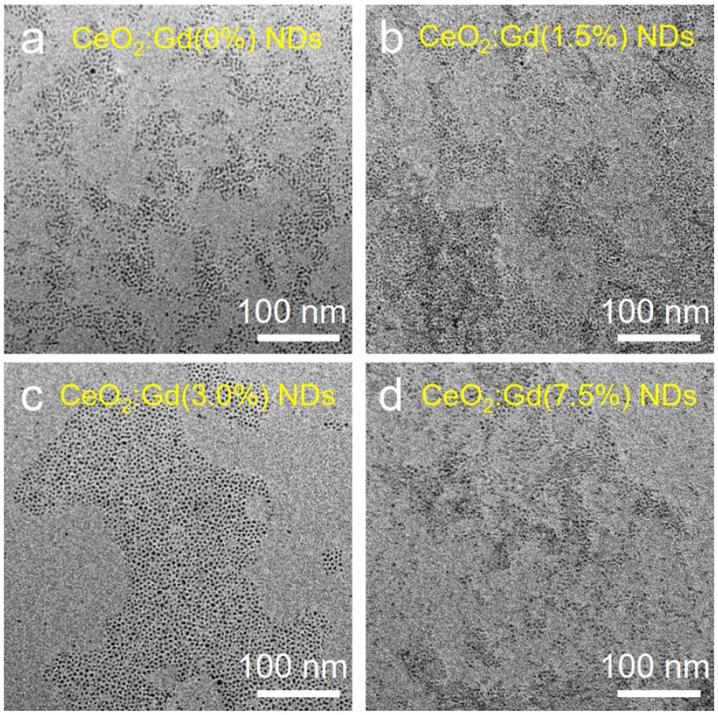

Fig. S2. TEM imaging of different Gd doping of CeO_2 NDs synthesized under 140 °C. (a) CeO_2:Gd(0%) NDs. (b) CeO_2:Gd(1.5%) NDs. (c) CeO_2:Gd(3.0%) NDs. (d) CeO_2:Gd(7.5%) NDs.

Various Gd doping did not change the morphology and size of CeO_2 NDs (**Fig. S2**).

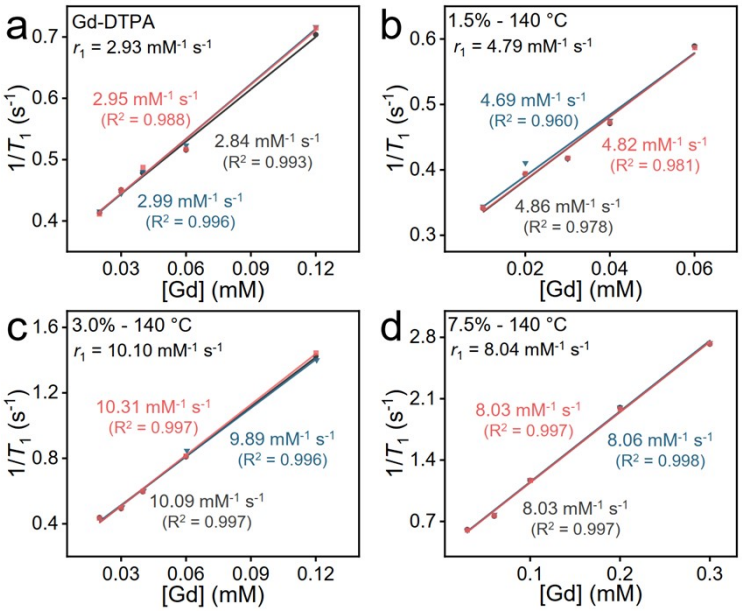

Fig. S3. (a) The $1/T_1$ values of Gd-DTPA solution with various Gd concentrations. The $1/T_1$ values of CeO_2:Gd(1.5%)@PSI_{OAm} (b), CeO_2:Gd(3.0%)@PSI_{OAm} (c) and CeO_2:Gd(7.5%)@PSI_{OAm} (d) solution with NDs prepared under 140 °C with virous concentrations. (7.0 T). Three different colored traces correspond to three different runs and r_1 value noted in figures was the averge relaxivity of three measurements.

Different Gd dopings (from 0% to 7.5%) influenced the longitudinal relaxation rate (r_1) of CeO_2:Gd@PSI_{OAm} nanoprobes and the highest value (10.17 $mM^{-1}s^{-1}$) was obtained with CeO_2: Gd(3.0%)@PSI_{OAm} under 7.0 T field strength (**Fig. S3**). As the Gd doping reached 7.5%, the r_1 was diminished to 8.05 $mM^{-1}s^{-1}$, which might be ascribed to the insufficient exposure of Gd atom at high doping amount.

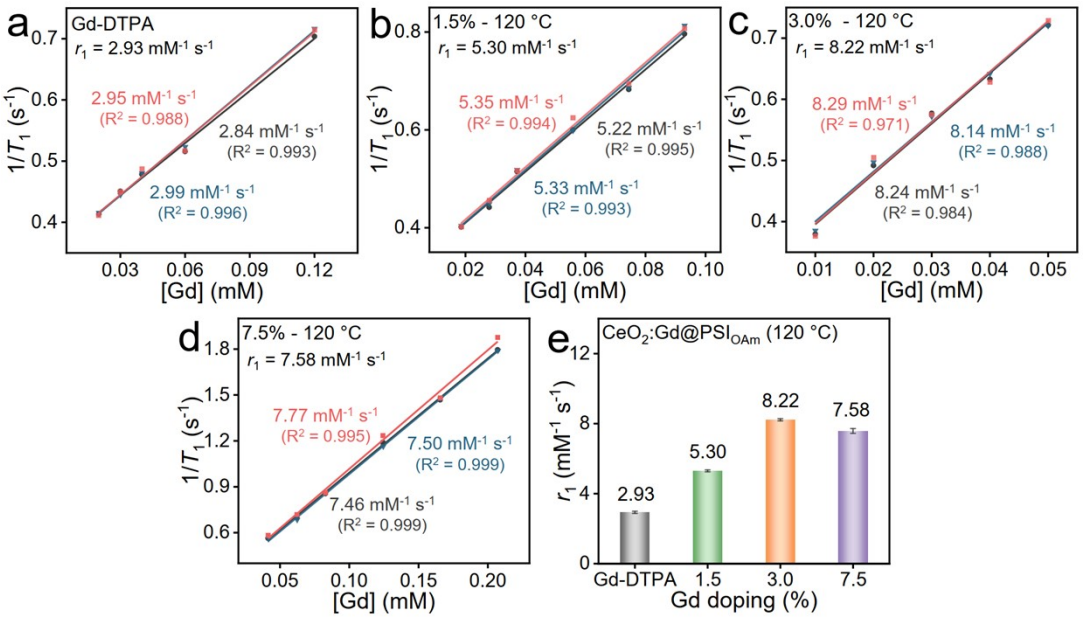

Fig. S4. (a) The $1/T_1$ values of Gd-DTPA solution with virous concentrations. The $1/T_1$ values of CeO_2:Gd(1.5%)@PSI_{OAm} (b), CeO_2:Gd(3.0%)@PSI_{OAm} (c) and CeO_2:Gd(7.5%)@PSI_{OAm} (d) solution with virous Gd concentrations. (e) The comparison of r_1 of CeO_2:Gd@PSI_{OAm} with CeO_2:Gd NDs prepared under 120 °C (7.0 T). Three different colored traces correspond to three different runs and r_1 value noted in figures was the averge relaxivity of three measurements.

The similar volcanic-trend also occurred to CeO_2:Gd NDs synthesized under 120 °C, suggesting the universal phenomena in Gd-doped inorganic nanoprobes (**Fig. S4**).

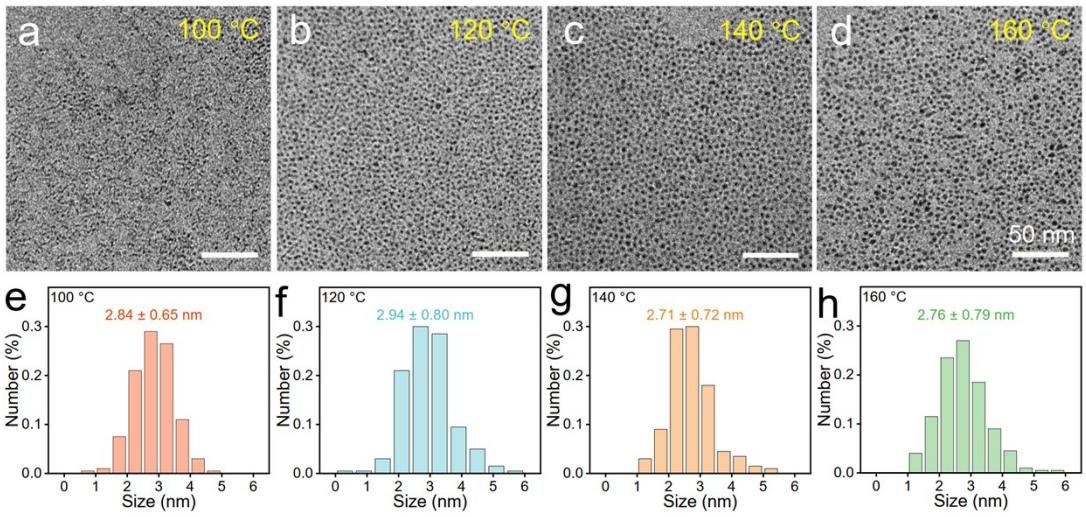

Fig. S5. TEM imaging and TEM observed size distribution of CeO_2:Gd(3.0%) NDs obtained under different temperatures: (a, e) 100 °C, (b, f) 120 °C, (c, g) 140 °C and (d, h) 160 °C.

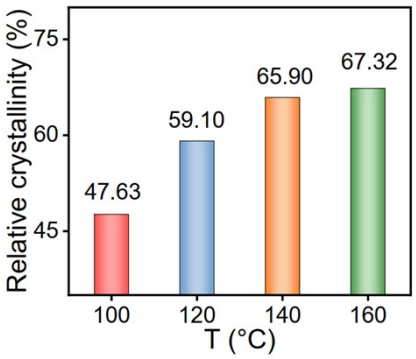

Fig. S6. The relative crystallinity of NDs (synthesized under different temperatures) obtained from XRD patterns calculated by MDI Jade 6 software.

The relative crystallinity (RC) can be calculated by MDI Jade 6 software and the corresponding formula was as follows.[3]

Relative crystallinity (RC) = crystalline area / (crystalline area + amorphous area) × 100%

We selected the (111), (220) and (311) facets of each sample as the main crystalline peaks to calculate the RC so as to reduce the influence of spectrogram noise. As shown in **Fig.S6**, the relative crystallinity increased along with increase of the synthetic temperatures of NDs.

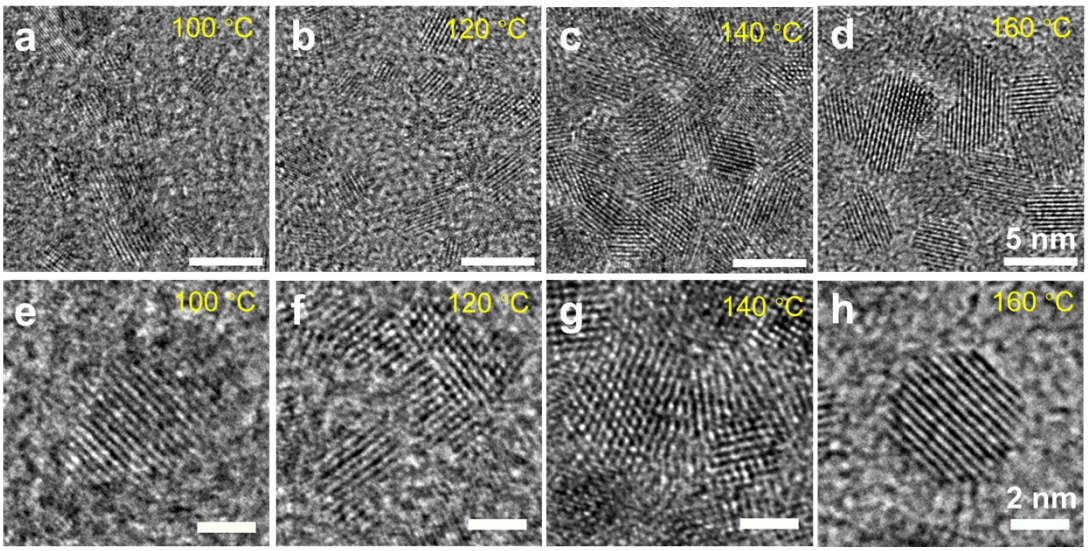

Fig. S7. HRTEM of CeO_2:Gd(3.0%) NDs obtained under different temperatures: (a,e) 100 °C, (b, f) 120 °C, (c, g) 140 °C and (d, h) 160 °C.

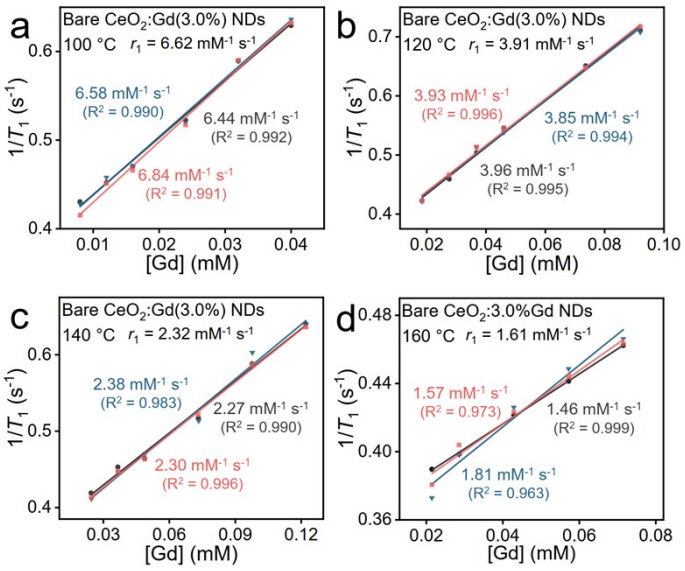

Fig. S8. The $1/T_1$ values of bare CeO_2:Gd (3.0%) NDs synthesized under different temperatures (a-d: 100 °C, 120 °C, 140 °C and 160 °C) with various Gd concentrations (7.0 T). Three different colored traces correspond to three different runs and the r_1 value noted in figure was the averge relaxivity of three measurements.

It was speculated the crystallinity degree of NDs may affect the relaxation performance of CeO_2:Gd(3.0%)@PSI_{OAm}. In order to demonstrate such assumption, we removed the OAm/OA ligands on the NDs and measured the r_1 of bare CeO_2:Gd(3.0%) NDs. Clearly, the r_1 values reduced stepwise along with the rise of temperature (**Fig. S8**), where the CeO_2:Gd(3.0%) NDs prepared under 100 °C displayed the best relaxivity. According to the Solomon-Bloembergen-Morgan (SBM) theory[4], the r_1 values of bare CeO_2:Gd(3.0%) NDs obtained under different temperatures were determined by the availability of the paramagnetic ions. The increased crystallinity of CeO_2:Gd(3.0%) NDs at high temperature might restrict the exposure of Gd atom, accordingly, impairing the relaxation performance, in line with the changes of the measured r_1.

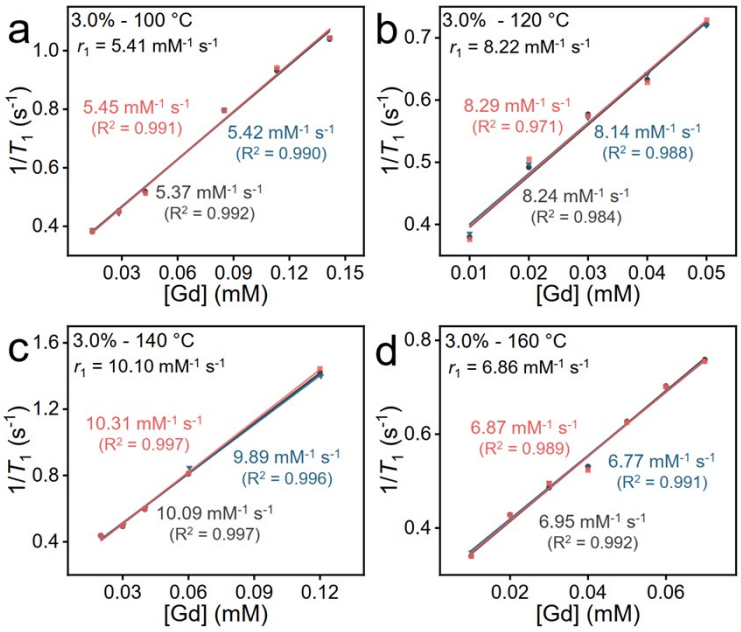

Fig. S9. The $1/T_1$ values of CeO_2:Gd(3.0%)@PSI_{OAm} nanocomposites with CeO_2:Gd(3.0%) NDs prepared under different temperatures (a-d: 100 °C, 120 °C, 140 °C and 160 °C) with various Gd concentrations (7.0 T). Three different colored traces correspond to three different runs and the r_1 noted in figures was the averge relaxivity of three measurements.

For the CeO_2:Gd(3.0%) NDs modified with amphilic polymer PSI_{OAm}, the r_1 changes did not follow the same trend as that of bare CeO_2:Gd(3.0%) NDs (**Fig. S8**), that is, the sample CeO_2:Gd(3.0%)@PSI_{OAm} with CeO_2:Gd(3.0%) NDs prepared under 140 °C exhibited the highest r_1 value (**Fig. S9**). The r_1 enhancement was such significant that it exceeded the enhancement *via* crystallinity engineering (bare CeO_2:Gd(3.0%) NDs prepared under 100 °C with low crystallinity), which implied that surface modification could also contribute to r_1 enhancement.

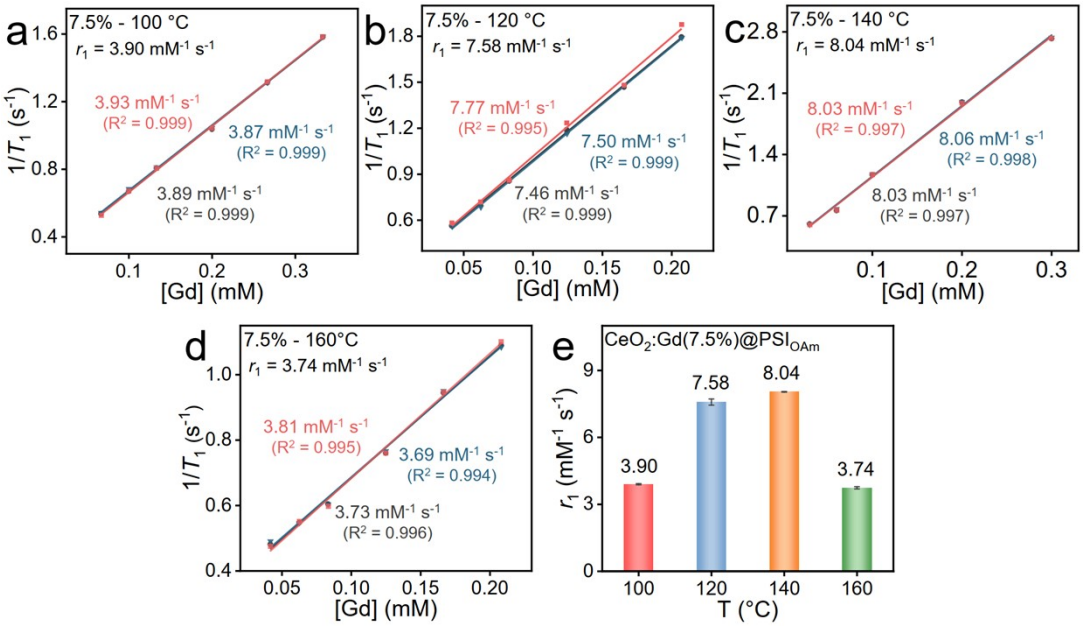

Fig. S10. The $1/T_1$ values of CeO_2:Gd(7.5%)@PSI_{OAm} nanocomposites with CeO_2:Gd(7.5%) NDs prepared under different temperatures (a-d: 100 °C, 120 °C, 140 °C and 160 °C) with virous Gd amounts. (e) The comparison of r_1 of CeO_2:Gd(7.5%)@PSI_{OAm} nanocomposites with CeO_2:Gd(7.5%) NDs prepared in different temperatures. (7.0 T) Three different colored traces correspond to three different runs and the r_1 noted in figures was the averge relaxivity of three measurements.

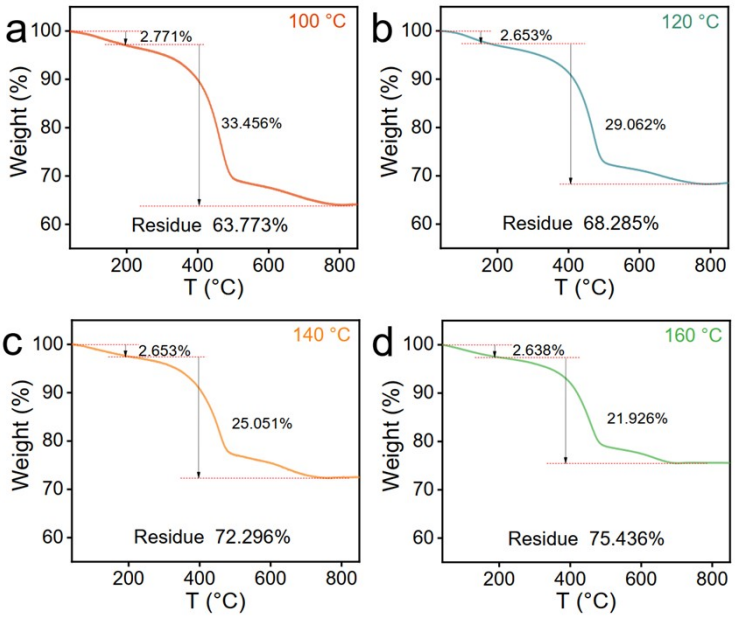

Fig. S11. The TGA values of CeO_2:Gd(3.0%) NDs synthesized under different temperatures ((a) 100°C, (b) 120°C, (c) 140°C and (d) 160°C).

The thermogravimetric analysis (TGA) illustrated the weight loss of hydrophobic NDs gradually decreased with the increase of temperature (**Fig. S11**), implying the surface ligands for NDs at low temperature was required more than that under high temperature. Moreover, the interaction between ligands and NDs was reflected by DTG curves(**Fig. 2e**), which suggested that stronger interaction existed between ligands and NDs acquired at low temperature. Thus, it was reasoned that for NDs with poor crystallinity, more capping ligands were needed, which in turn, required more polymer PSI_{OAm} to render enough hydrophilicity, thus, leading to significant increase of the overall hydrodynamic size. However, the increased hydrodynamic size impeded the relaxation of paramagnetic core toward outer sphere proton. Thus, it is a trade-off between crystallinity and the surface ligand coating. Ideally, to improve the overall relaxivity, we anticipated that the nanoprobes should exhibit poor crystallinity, good hydrophilicity while maintaining large rotation time.

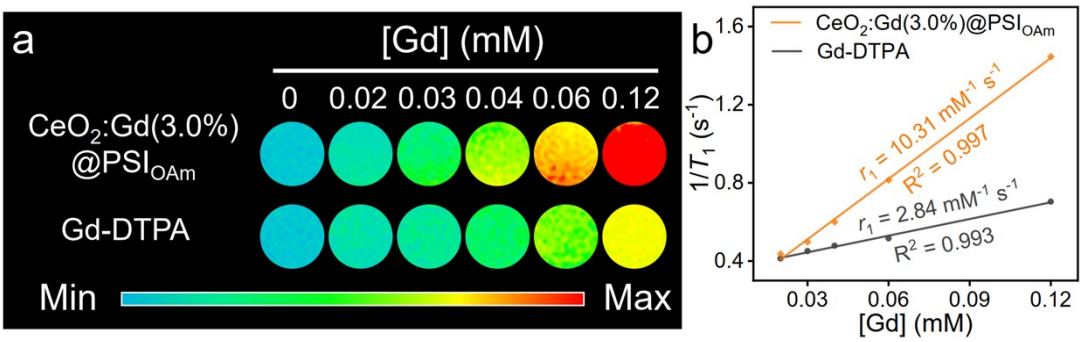

Fig. S12. (a) T_1-weighted ^{1}H MRI of CeO_2:Gd(3.0%)@PSI_{OAm} solution and commercial CA Gd-DTPA with various Gd amounts. (b) The $1/T_1$ values of CeO_2:Gd(3.0%)@PSI_{OAm} solution and Gd-DTPA with various Gd concentrations. (7.0 T)

We explored the capability of CeO_2:Gd(3.0%)@ PSI_{OAm} with NDs prapared under 140 °C for *in vitro* MRI. As shown in **Fig. S12**, The T_1-weighted ^{1}H MRI displayed clearly brightening contrast enhancement along with increase of Gd concentration. While the T_1-weighted MRI of commercial Gd-DTPA hardly changed, suggesting the great potential for *in vivo* MRI.

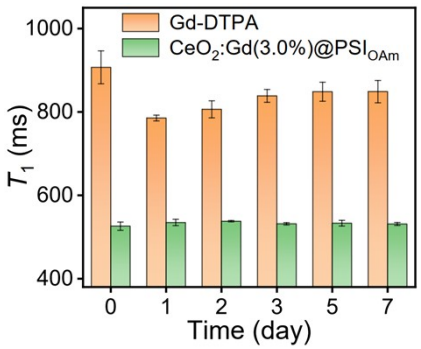

Fig. S13. Time-dependent relaxation time of Gd-DTPA and CeO_2:Gd(3.0%)-TMB@PSI_{OAm} treated with 5 equivalent of Zn^{2+}. (n = 3)

As shown in **Fig. S13**, even treated with 5 equivalents of Zn^{2+}, the relaxation time of CeO_2:Gd(3.0%)-TMB@PSI_{OAm} maintained stable for more than 7 days, while the T1 of commercial Gd-DTPA varied dramatically soon after addition of Zn^{2+}, indicating the CeO_2:Gd(3.0%)-TMB@PSI_{OAm} probes was resistant to metal competitive binding.

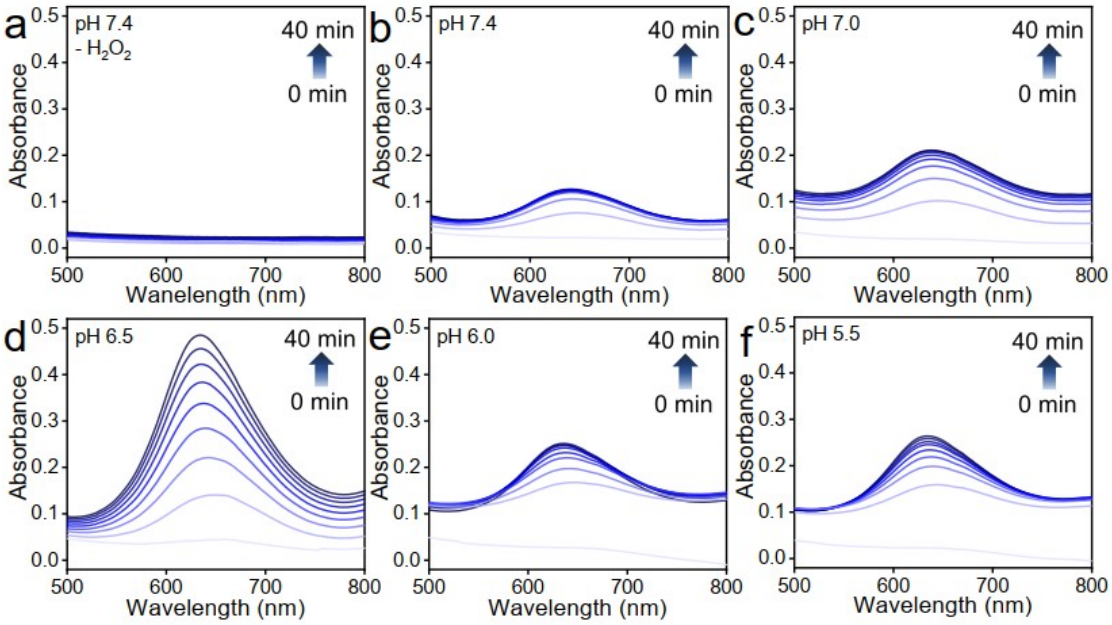

Fig. S14. TMB absorption spectra of CeO_2:Gd(0%)@PSI_{OAm} in the presence of 1 mM H_2O_2 in different pH ((a) pH 7.4 without H_2O_2; (b) pH 7.4; (c) pH 7.0; (d) pH 6.5; (e) pH 6.0; (f) pH 5.5). The concentration of TMB was 0.1 mg/mL.

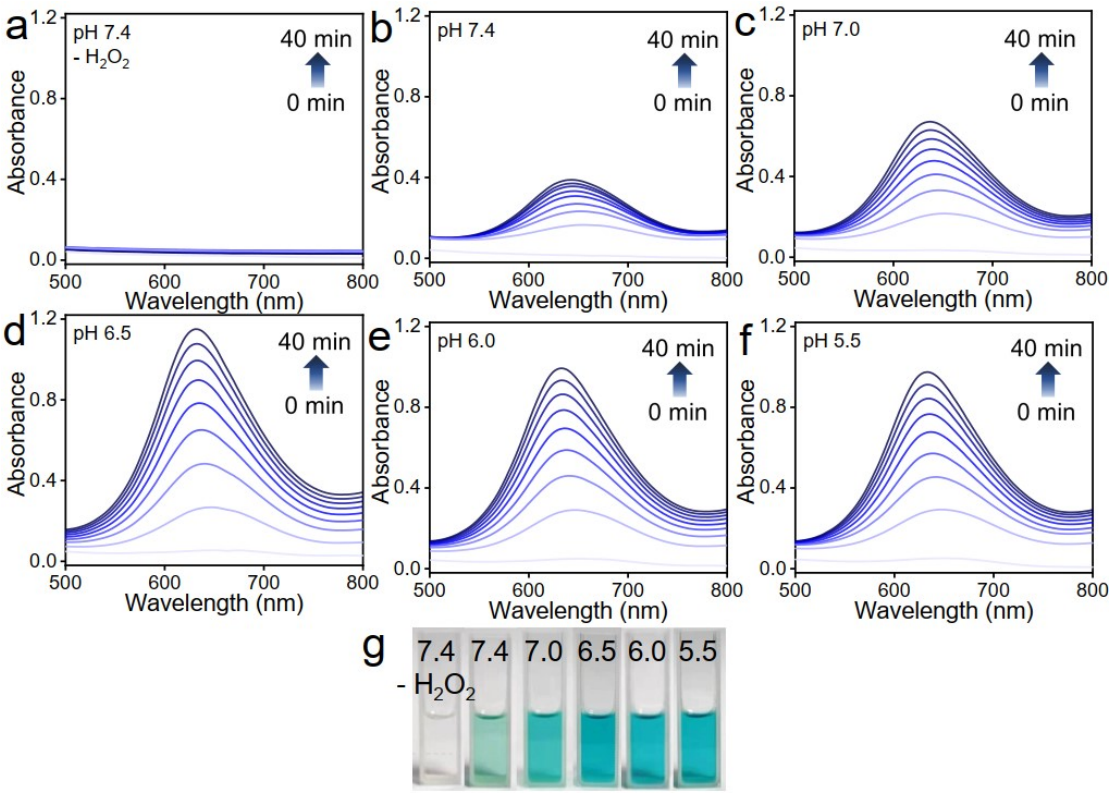

Fig. S15. TMB absorption spectra of CeO_2:Gd(3.0%)@PSI_{OAm} in the presence of 1 mM H_2O_2 in different pH ((a) pH 7.4 without H_2O_2; (b) pH 7.4; (c) pH 7.0; (d) pH 6.5; (e) pH 6.0; (f) pH 5.5) and the photograph of solutions at 40 min (g). The concentration of TMB was 0.1 mg/mL.

CeO_2:Gd(0%)@PSI_{OAm} and CeO_2:Gd(3.0%)@PSI_{OAm} exhibited good peroxidase-like activity to oxidize TMB into oxidized TMB (oxTMB) in the presence of H_2O_2, accompanied by a color change from colorless to blue. As shown in **Fig. S14**, the absorption of TMB at 632 nm gradually enhanced for CeO_2: Gd(0%)@PSI_{OAm} in the presence of H_2O_2 with optimal pH of 6.5, indicating the dual responsive features (pH and H_2O_2) of CeO_2, which was preferable in view of the slight acidic and oxidative conditions at tumor sites. Interestingly, under identical conditions, CeO_2:Gd(3.0%)@PSI_{OAm} displayed higher catalytic activities than that of CeO_2:Gd(0%)@PSI_{OAm} (**Fig. S15).**

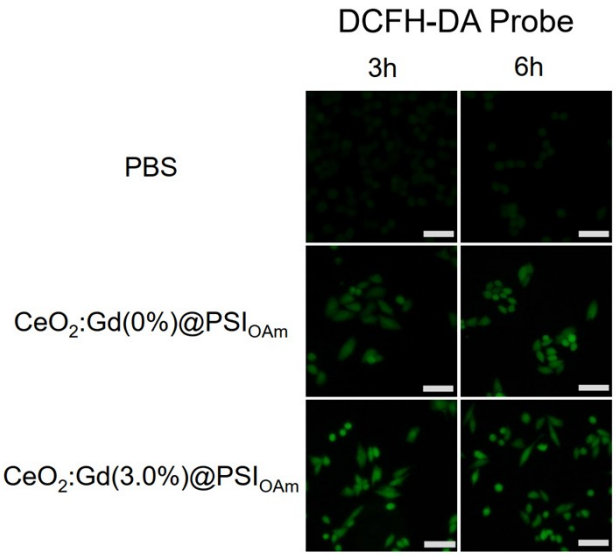

Fig. S16. Fluorescence imaging of 4T1 cells treated with DCFH-DA probe after co-incubated with PBS, CeO_2:Gd(0%)@PSI_{OAm} and CeO_2:Gd(3.0%)@PSI_{OAm} for 3 h and 6 h, respectively. (Scale bar: 20 μm)

To verify the peroxidase-like activity in cellular level, we utilized a ROS indicator 2,7-dichlorodihydrofluorescein diacetate (DCFH-DA, 10 μM) to monitor the production of ROS at cellular level. As shown in **Fig. S16**, the 4T1 cells incubation with CeO_2:Gd(3.0%)@PSI_{OAm} exhibited the most significant enhancement of green fluorescence, indicating the enhanced generation of ROS in CeO_2:Gd(3.0%)@PSI_{OAm} group.

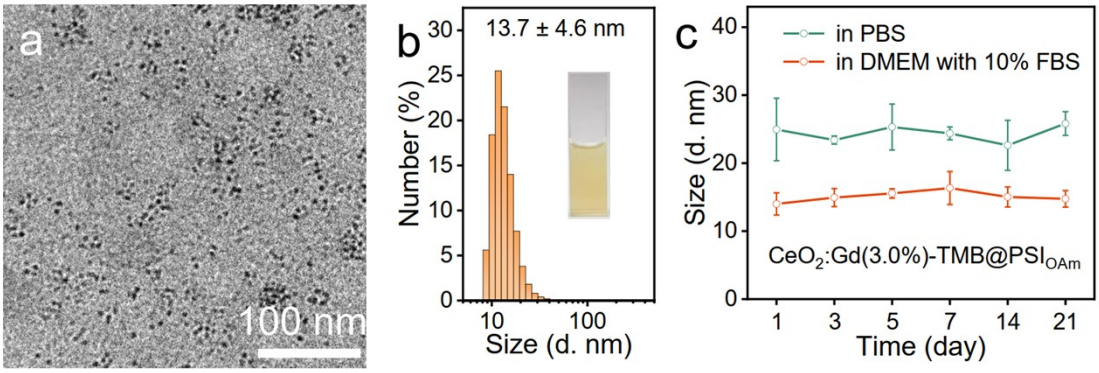

Fig. S17. (a) TEM image and (b) DLS size distribution and photograph of CeO_2:Gd(3.0%)-TMB@PSI_{OAm}. (c) The stability of CeO_2:Gd(3.0%)-TMB@PSI_{OAm} in PBS and DMEM with 10% FBS for 21 days. (n = 3)

As shown in **Fig. S17,** CeO_2:Gd(3.0%)-TMB@PSI_{OAm} displayed similar morphology and particle size as that of CeO_2:Gd(3.0%)@PSI_{OAm}. CeO_2:Gd(3.0%)-TMB@PSI_{OAm} solution can be stable in PBS buffer and DMEM with 10% FBS for 21 days, implying the satisfied biological stability.

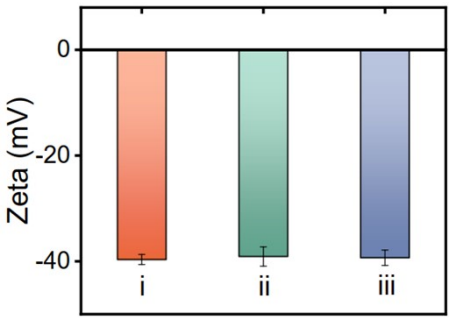

Fig. S18. The zeta potential of different samples: (i) CeO_2:Gd(3.0%)@PSI_{Oam}, (ii) CeO_2:Gd(3.0%)-TMB@PSI_{OAm} and (iii) CeO_2:Gd(3.0%)-TMB@PSI_{OAm} incubated with H_2O_2.

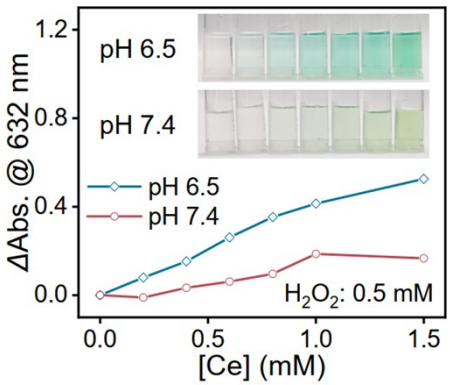

Fig. S19. The increased absorption intensity of CeO_2:Gd(3.0%)-TMB@PSI_{OAm} nanocomposites at 632 nm for different concentrations of CeO_2:Gd(3.0%)-TMB@PSI_{OAm} in the presence of 0.5 mM of H_2O_2 at pH 6.5 and 7.4.

Along with the increase concentration of CeO_2:Gd(3.0%)-TMB@PSI_{OAm} nanocomposites, the absorption (**Fig. S19**) and PA signal (**Fig. 3d**) sharply enhanced at pH 6.5 while the signal rose slowly and tended to be constant under pH 7.4. Such results suggested the PA signal increased in a pH-dependent manner.

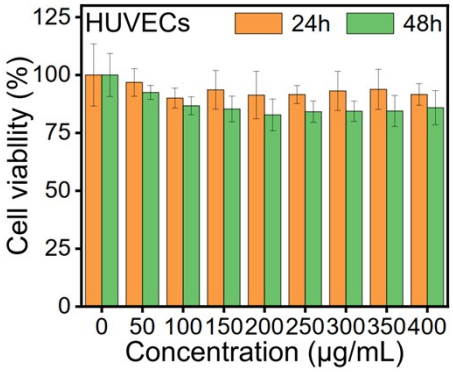

Fig. S20. Cytotoxicity of CeO_2:Gd(3.0%)-TMB@PSI_{OAm}. (n = 6)

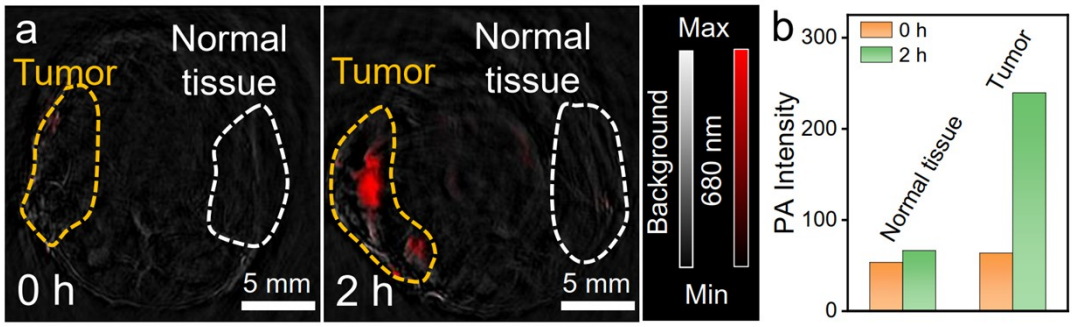

Fig. S21. (a) The PA imaging of mice after intratumor and subcutaneous injection of CeO_2:Gd(3.0%)-TMB@PSI_{OAm}. (b) The comparison of PA intensity at tumor and normal tissue sites, respectively under different time intervals.

The slight time delay may have originated from the response properties of PAI as revealed by results shown in **Fig. S21**. After intra-tumor and subcutaneous injection for 2 h, the PA signal intensity at tumor site (left) was clearly stronger than that in normal tissues (right) (**Fig. S21**), which proved CeO_2:Gd(3.0%)-TMB@PSI_{OAm} possessed excellent TME responsive PAI performance.

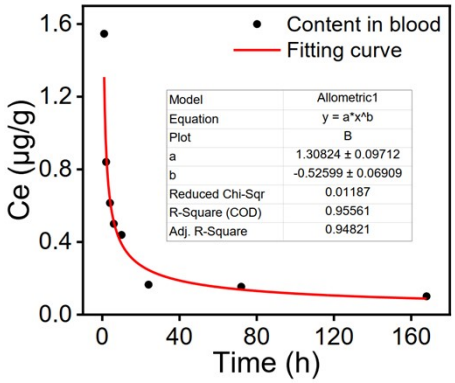

Fig. S22. The fitting curve of time-dependent distribution of CeO_2:Gd(3.0%)-TMB@PSI_{OAm} in blood within 7 days.

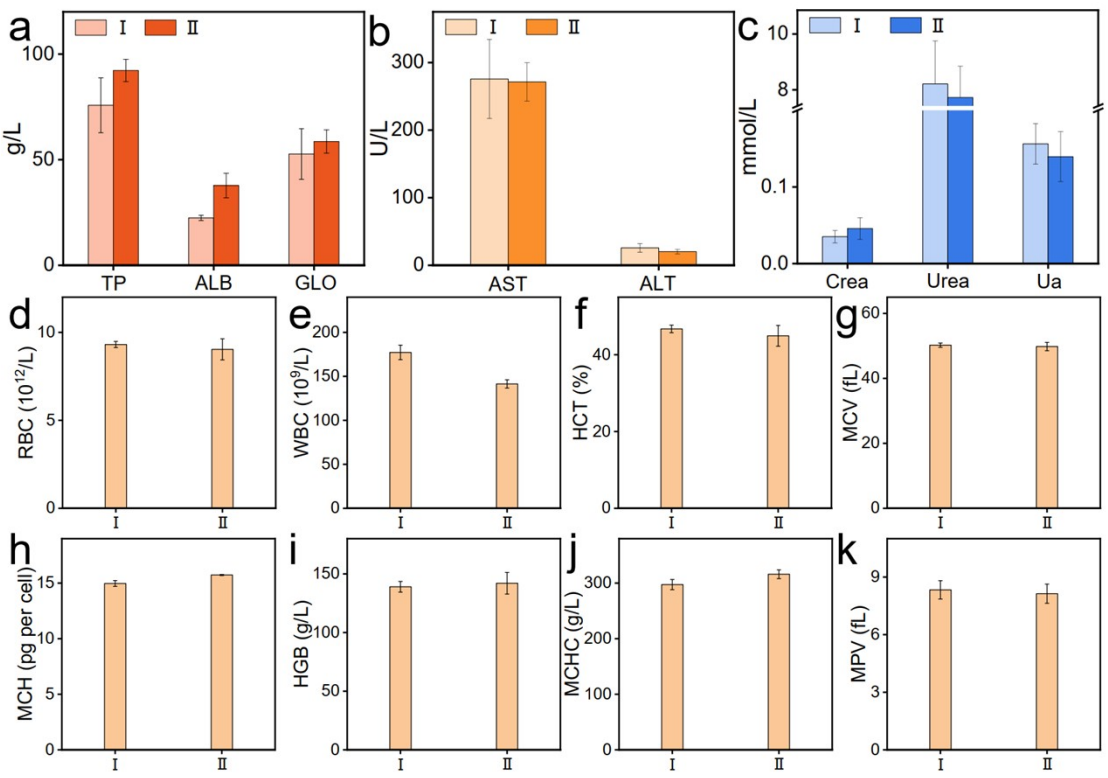

Fig. S23. Biological toxicity study. 4T1 tumor-bearing mice with *i.v.* injection of different samples (I and II refer to the groups of PBS and CeO_2:Gd(3.0%)-TMB@PSI_{OAm} respectively) were sacrificed for blood collection. The comparison of important liver function indicator, namely (a) total protein (TP), albumin (ALB) and globulin (GLO) levels; (b) aspartate aminotransferase (AST), alanine aminotransferase (ALT) levels. (c) The comparison of kidney function indicator including creatinine (Crea), urea nitrogen (Urea) and uric acid (Ua) levels. Blood routine indicators containing (d) red blood cells (RBC), (e) white blood cells (WBC), (f) hematocrit (HCT), (g) mean corpuscular volume (MCV), (h) mean corpuscular hemoglobin (MCH), (i) hemoglobin (HGB), (j) mean corpuscular hemoglobin concentration (MCHC) and (k) mean platelet volume (MPV) levels. (n = 3)

Blood index examination suggested excellent biosafety without any observable harm to liver and renal function (**Fig. S23**).

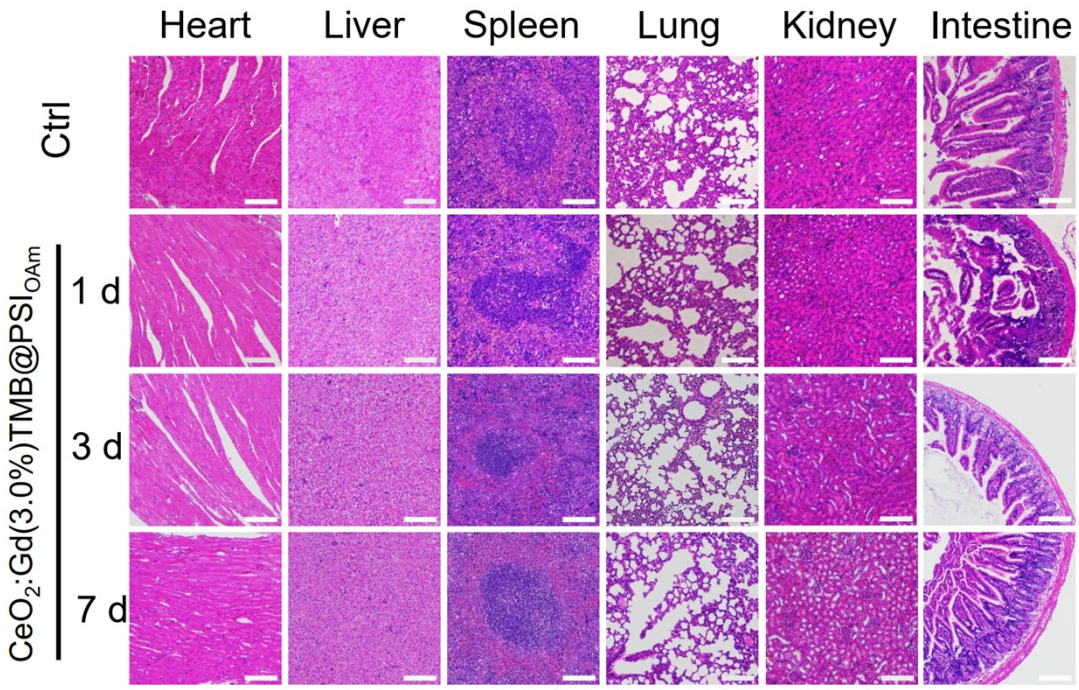

Fig. S24. Hematoxylin-eosin (H&E) staining imaging of major organs (heart, liver, spleen, lung, kidney and intestine) of 4T1-bearing mice and that injected with CeO_2:Gd(3.0%)-TMB@PSI_{OAm} solution for 1 and 3 days, respectively. (Scale bar: 100 μm.)

There was no pathological changes occurred for major organs after i.v injection of CeO_2:Gd(3.0%)-TMB@PSI_{OAm}, as suggested by H&E staining (**Fig. S24**), demonstrating the satisfied biosafety.

References

1. S. Huang, M. Bai and L. Wang, *Scientific Reports*, 2013, **3**, 2023-2027.
2. S. Huang, S. Peng, Y. Li, J. Cui, H. Chen and L. Wang, *Nano Research*, 2015, **8**, 1932-1943.
3. K. Frost, D. Kaminski, G. Kirwan, E. Lascaris and R. Shanks, *Carbohydrate Polymers*, 2009, **78**, 543-548.
4. Z. Zhou, L. Yang, J. Gao and X. Chen, *Adv. Mater.*, 2019, **31**, NO. 1804567.